Proceedings of Global Power and Propulsion Society
ISSN-Nr: 2504-4400
Beijing Conference 2019
16th – 18th September, 2019
www.gpps.global

GPPS-BJ-2019-0098

THERMODYNAMIC ANALYSIS OF VARIOUS COMBINED SOFC-SCO_2 BRAYTON CYCLE SYSTEM LAYOUTS

Liu XIA
Key Laboratory for Thermal Science and Power Engineering of Ministry of Education, Department of Energy and Power Engineering, Tsinghua University
xia-l18@mails.tsinghua.edu.cn
Beijing, China

Xuesong LI
Key Laboratory for Thermal Science and Power Engineering of Ministry of Education, Department of Energy and Power Engineering, Tsinghua University
xs-li@tsinghua.edu.cn
Beijing, China

Jian SONG
Clean Energy Processes Laboratory, Department of Chemical Engineering, Imperial College London
jian.song@imperial.ac.uk
London, United Kingdom

Xiaodong REN
Key Laboratory for Thermal Science and Power Engineering of Ministry of Education, Department of Energy and Power Engineering, Tsinghua University
rxd@mail.tsinghua.edu.cn
Beijing, China

Chunwei GU
Key Laboratory for Thermal Science and Power Engineering of Ministry of Education, Department of Energy and Power Engineering, Tsinghua University
gcw@mail.tsinghua.edu.cn
Beijing, China

ABSTRACT

Solid oxide fuel cell (SOFC) has been considered to be a promising power generation technology due to that the high-temperature exhaust gas of SOFC can be used as another heat source for a bottoming cycle to increase the overall efficiency. This study presents a performance analysis for a combined power generation system consisting of an SOFC and a simple recuperated S-CO_2 Brayton cycle. Four system layouts based on different exhaust utilization ways are analysed and compared in this study. The results indicate that the S-CO_2 Brayton cycle can be a promising way for waste-heat recovery of SOFC. The system layout with six heat exchangers and two burners shows the highest output power while the system layout with seven heat exchangers and only one burner shows the highest thermal efficiency.

INTRODUCTION

The overuse of fossil fuels has brought on a series of problems and challenges, such as energy shortage and environmental deterioration. Consequently, it has rapidly increased the interest in the new power generation technologies to improve the energy conversion efficiency and reduce carbon emissions. Solid oxide fuel cell (SOFC) has been considered to be a promising technology due to its high efficiency, relatively low fuel selectivity, and environmental friendliness. In addition, the energy security, reliability, low operating and maintenance cost, and constant power production of SOFC make it potential to be used in various applications such as cogeneration systems, trigeneration systems, and small scale residential applications. SOFC is also a strong contender for transportation application including cars and commercial vessels due to its compatibility with hydrocarbon fuels [1-3]. The SOFC produces electricity from chemical components at a high operating temperature, thus the high-temperature exhaust gas of SOFC can be further recovered to increase the overall efficiency.

Among various technologies for utilizing this heat, directly coupled SOFC/gas turbine (GT) hybrid systems have been studied most extensively. The GT provides pressurized and preheated air to SOFC while the exhaust gas of SOFC directly drive the GT to produce additional power. Ali Volkan Akkaya et al. [4] conducted an exergetic performance analysis on the combination of an SOFC and GT in a combined heat and power (CHP) system for distributed applications. Wolfgang Winkler and Hagen Lorenz [5-6] performed the design study of mobile applications with SOFC-GT modules. The results revealed that the integration of an SOFC-GT power system was promising to be exploited provided the

available space in a mid-class car. E. Gholamian and V. Zare [7] proposed two SOFC/GT hybrid systems using organic Rankine cycle (ORC) and Kalina cycle (KC) as bottoming cycles. The results showed that the temperature of exhaust gas from the SOFC/GT system was still high enough to be used for power generation in a proper system, and the SOFC/GT-ORC had a better thermodynamic performance and significantly lower operating pressure compared to the SOFC/GT-KC system. Shiqi Zhang et al. [8] proposed an integrated modelling and optimization framework for a combined power system comprising SOFC, GT and ORC. The result indicated that an electricity efficiency of 66.27% and a CHP efficiency of 88.43% could be achieved by the integrated system.

Indirectly coupled system of SOFC with bottoming cycles is another option for waste-heat utilization. The advantage of such systems lies in that generally these atmospheric plants are easier to manage [9]. Masoud Rokni [10] conducted thermodynamic analysis of an integrated SOFC with an ORC cycle and evaluated the influence of different pre-reforming types on the thermal efficiency. Ali Volkan Akkaya and Bahri Sahin [11] developed a mathematical model to simulate the SOFC-ORC combined system under steady-state conditions and the effects of variation of main design parameters were investigated under wide range. Based on the investigated design parameter conditions, thermal efficiency can be increased by recovering SOFC waste heat through ORC.

Recently, the supercritical carbon dioxide Brayton cycle has emerged as one promising technology due to its high efficiency and has been developed for a wide range of energy conversion applications [12-14]. The S-CO_2 cycle can be used for various heat sources including high temperature fuel cells [15]. Seong Jun Bae et al. [16] conducted preliminary studies of comparing performance of various S-CO_2 cycles for a power conversion system of a Molten Carbonate Fuel Cell. The S-CO_2 cycle can be another attractive bottoming option for SOFC. However, the investigation on combined SOFC-SCO_2 Brayton cycle system is very limited see S.I. Schöffer [17].

In this study, the performance analysis for an indirectly coupled system consisting of an SOFC and a simple recuperated S-CO_2 Brayton cycle is presented. The given data of the SOFC operating condition by Ali Volkan Akkaya and Bahri Sahin[11] are used. Four system layouts based on different exhaust utilization ways are selected as candidates. As Ali Volkan Akkaya and Bahri Sahin[11] believe that ORC can be an attractive bottoming option for SOFC, performances of each system proposed in this study as well as the SOFC-ORC system proposed in [11] are compared in terms of the thermal efficiency, output power, and net electricity of the combined system.

THERMODYNAMIC MODELING AND ANALYSIS OF VARIOUS LAYOUTS

The four basic configurations of the combined SOFC-SCO_2 Brayton cycle systems considered in this study are shown in Figure 1. The considered fuel cell is the same as the tubular SOFC design explained in the literature [11], the modelling of which has already been validated with the published experimental test data of tubular SOFC developed by Siemens Westinghouse[18]. In each combined system, the SOFC produces electrical power through electrochemical conversion of the fuel chemical energy. The waste heat of the SOFC is discharged in the form of exhaust gas and used as heat source of the S-CO_2 Brayton cycle for additional electrical power generation. The operating conditions of SOFC in the proposed four systems are the same. The simple recuperated Brayton cycle is selected as the bottoming cycle.

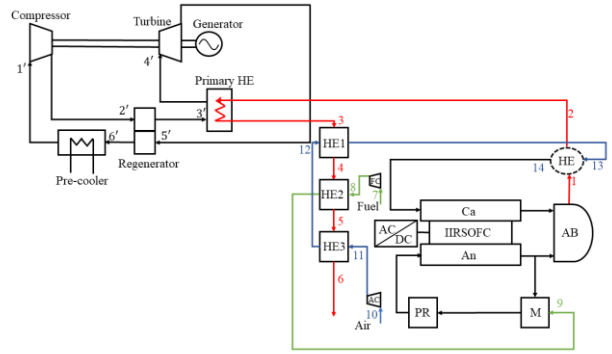

(a) Layout 1: Combined SOFC-S-CO_2 system without extra fuel

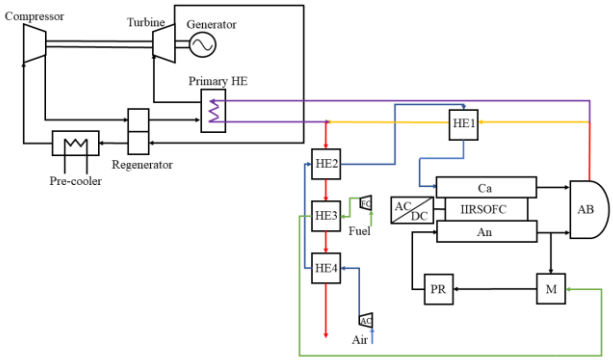

(b) Layout 2: Combined SOFC-S-CO_2 system with an additional HE and no extra fuel

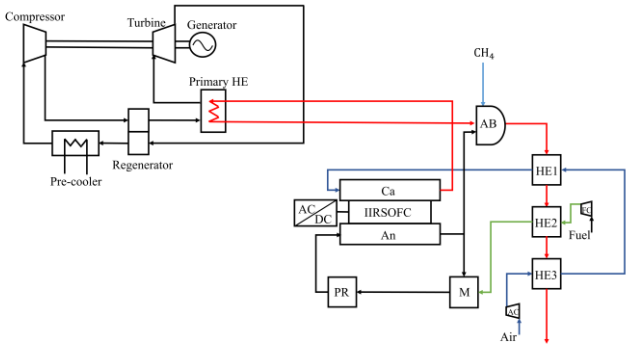

(c) Layout 3: Combined SOFC-S-CO_2 system with extra fuel

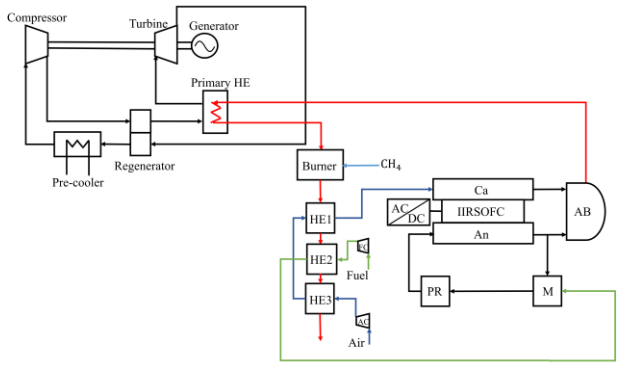

(d) Layout 4: Combined SOFC-S-CO_2 system with an additional burner and extra fuel

Figure 1. SOFC-SCO_2 Brayton cycle combined system layouts.

In the SOFC section, methane (selected as fuel) and air are pressurized respectively by fuel compressor (FC) and air compressor (AC). Then they are preheated before entering the reformer (IIRSOFC). The An (anode) gas is partly recirculated and then mixed with fuel in the mixer (M). The mixed gas is reformed in the pre-reformer (PR) where hydrogen (H_2), carbon monoxide (CO) and carbon dioxide (CO_2) are produced. Respectively, the reformed gas and air flow into An and Ca (cathode) where the electrochemical reaction takes place. Electricity is produced in this part, accompanied with heat. Besides, not all fuel is utilized in the fuel cell, hence the H_2 and CO in An exhaust can be combusted with depleted air in the afterburner (AB) to raise the temperature. Finally, the exhaust gas serves as the heat source for the S-CO_2 section. Among various S-CO_2 cycle layouts, taking simplicity into consideration, the simple recuperated Brayton cycle is selected in this paper. The S-CO_2 from the pre-cooler is first compressed to a high-pressure state by the compressor, then preheated by the exhaust gas from the SOFC in the primary heat exchanger. Next, the high-temperature and high-pressure S-CO_2 expands in the turbine to drive the generator and produce power. The S-CO_2 from the turbine is cooled to the initial state by the regenerator and pre-cooler in series.

The way in which the fuel and air are preheated and the flow path of the exhaust gas vary in different layouts. In layout 1, the exhaust from An and Ca are mixed and burned in the AB, then flows into the heat exchanger (HE) to heat the preheated air further. Afterwards, the exhaust flows into the primary HE as the heat source for the S-CO_2 section. The exhaust from the primary HE flows through HE1, HE2, and HE3 in sequence to preheat the air and fuel. Unlike layout 1, the exhaust from AB in layout 2 is split into two parts. Stream1 flows into the primary HE as the heat source for the S-CO_2 section, while stream 2 flows into the HE 1 to heat the preheated air further. The ratio of the mass flow rate of stream 1 to stream 2 is called the split ratio. Then the two streams are mixed and flows through HE 2, HE 3 and HE 4 in sequence to preheat the air and fuel. In layout 3, the exhaust from An firstly serves as the heat source for S-CO_2 section. In the AB, the exhaust from the primary HE is mixed with the Ca exhaust. Extra fuel is added and reacted to achieve the required temperature. The exhaust from AB flows through HE 1, HE 2 and HE 3 to preheat the air and fuel. The system of layout 4 is much simpler, the exhaust from AB directly flows into the primary HE as the heat source for the S-CO_2 section. Then the exhaust flows into a burner and reacts with the extra fuel to reach the required temperature. Then the exhaust flows through HE 1, HE 2 and HE 3 to preheat the air and fuel.

In layout 1, the output power varies with the temperature of the preheated air from HE 1. Apparently, the output power of layout 2 varies with the split ratio and the maximum occurs with the highest split ratio. The output power of layout 3 and layout 4 is fixed.

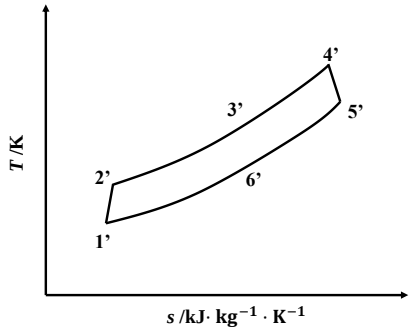

Figure 2. *T-s* diagram of simple recuperated Brayton cycle.

Figure 2 shows the *T-s* diagram of the simple recuperated Brayton cycle. Taking layout 1 for example, the thermal process can be described as follows.

In the S-CO_2 section, the consumed power in the compressor, W_{com}, is given by

$$W_{com} = \frac{\dot{m}_{S-CO_2} \cdot (h_{2's} - h_{1'})}{\eta_{com}}, \quad (1)$$

Where $h_{2's}$ is the S-CO_2 isentropic enthalpy after being pressurized in the compressor, and η_{com} is the compressor efficiency.

The heat transfer rate in the regenerator, $\dot{Q}_{reg}$, is given by

$$\dot{Q}_{reg} = \dot{m}_{S-CO_2} \cdot (h_{3'} - h_{2'}) = \dot{m}_{S-CO_2} \cdot (h_{5'} - h_{6'}), \quad (2)$$

The effectiveness of regenerator is defined as

$$\varepsilon = \frac{h_{5'} - h_{6'}}{h_{5'} - h_{6's}(T_{2'}, P_{6'})}, \quad (3)$$

where $h_{6's}(T_{2'}, P_{6'})$ is calculated based on the assumption that the temperature of the hot S-CO_2 stream leaving the regenerator reaches the temperature of state $2'$.

The heat transfer rate in the primary heat exchanger, $\dot{Q}_{PHE}$, is given by

$$\dot{Q}_{PHE} = \dot{m}_{HS} \cdot c_{p,HS} \cdot (T_{HS,in} - T_{HS,out}) = \dot{m}_{S-CO_2} \cdot (h_{4'} - h_{3'}), \quad (4)$$

where $c_{p,HS}$ is the average specific heat capacity of the heat source, and $T_{HS,in}$ and $T_{HS,out}$ are respectively its inlet and outlet temperatures.

The power output of the turbine, W_{tur}, is given by

$$W_{tur} = \dot{m}_{S-CO_2} \cdot (h_{4'} - h_{5's}) \cdot \eta_{tur}, \quad (5)$$

where $h_{5's}$ is the S-CO_2 isentropic enthalpy at the turbine outlet and η_{tur} is the turbine efficiency.

The heat transfer rate in the pre-cooler, $\dot{Q}_{pre\text{-}c}$, is given by

$$\dot{Q}_{pre-c} = \dot{m}_{S-CO_2} \cdot (h_{6'} - h_{1'}). \quad (6)$$

The net power output of the system, W_{net}, is

$$W_{net} = W_{tur} - W_{com}. \quad (7)$$

The thermal efficiency of the S-CO_2 system, η_{net}, can be calculated by

$$\eta_{net} = \frac{W_{net}}{\dot{Q}_{PHE}}. \quad (8)$$

In the SOFC section, the heat transfer rate in the HE, $\dot{Q}_{\mathrm{HE}}$, is given by

$$\dot{Q}_{HE} = \dot{m}_{HS} \cdot (h_1 - h_2) = \dot{m}_{air} \cdot (h_{14} - h_{13}), \quad (9)$$

where $\dot{m}_{HS}$ and $\dot{m}_{air}$ represent the mass flow rate of the exhaust gas and air from AB and HE1 respectively.

Then the exhaust gas flows into the primary HE in the S-CO_2 section as the heat source. The heat transfer rate in the HE1 provided by the exhaust gas from primary HE is given by

$$\dot{Q}_{HE1} = \dot{m}_{HS} \cdot (h_3 - h_4) = \dot{m}_{air} \cdot (h_{13} - h_{12}). \quad (10)$$

The heat transfer rate in the HE 2 is

$$\dot{Q}_{HE2} = \dot{m}_{HS} \cdot (h_4 - h_5) = \dot{m}_{fuel} \cdot (h_9 - h_8). \quad (11)$$

The heat transfer rate in the HE 3 is

$$\dot{Q}_{HE3} = \dot{m}_{HS} \cdot (h_5 - h_6) = \dot{m}_{air} \cdot (h_{12} - h_{11}). \quad (12)$$

Thermal analysis of layout 2, 3, and 4 is similar to layout 1. In layout 3 and layout 4, there is extra fuel added to the burner. Assume that all combustible compounds are fully oxidized in the burner, the following energy balance equations are employed to calculate the flowrate and temperature of the exhaust existing the burner [19]. In layout 3, the associated equations are given by

$$\dot{m}_{An} \cdot h_{An} + \dot{m}_{Ca} \cdot h_{Ca} + \dot{m}_{fuel} \cdot h_{fuel} = \dot{m}_{mix} \cdot h_{mix}, \quad (13)$$

$$\dot{m}_{An} + \dot{m}_{Ca} + \dot{m}_{fuel} = \dot{m}_{mix}, \quad (14)$$

where $\dot{m}_{An}$, $\dot{m}_{Ca}$, $\dot{m}_{fuel}$, and $\dot{m}_{mix}$ denote the mass flow rate of the exhaust from An flowing into the AB, the mass flow rate of the exhaust from the primary HE flowing into the AB, the mass flow rate of the extra added fuel and the mass flow rate of the exhaust existing the AB respectively, and h_{An}, h_{Ca}, h_{fuel}, and h_{mix} represent the relevant specific enthalpy. The temperature of the exhaust existing the AB is calculated according to its specific enthalpy. The equations for layout 4 are similar to equation (13) and (14).

Table 1. Basic parameters of the hybrid system.

Parameter	Value
Air mass flow	0.896 kg/s
Fuel mass flow	0.011 kg/s
Pressure of state 9	1.101 bar
Temperature of state 9	506.65 K
Pressure of state 14	1.101 bar
Temperature of state 14	1012.75 K
Compressor inlet temperature	305.15 K
Compressor inlet pressure	7.7 MPa
Turbine inlet pressure	20 MPa
Compressor efficiency	70%
Turbine efficiency	80%
Regenerator effectiveness	0.95
High pressure side of regenerator pressure loss	0.01
Low pressure side of regenerator pressure loss	0.015
Primary heat exchanger pressure loss	0.015
Pre-cooler pressure loss	0.02

Table 1 provides some basic parameters of the designed system. As the research objective is to explore the effects of different exhaust utilization ways, the states of fuel and air flowing into M and Ca respectively are kept constant. The REFPROP 8.0 database developed by NIST is adopted in the cycle calculations.

RESULTS AND DISCUSSION

As the operating condition of the SOFC section remains unchanged, the hybrid system performance is determined by the S-CO_2 section.

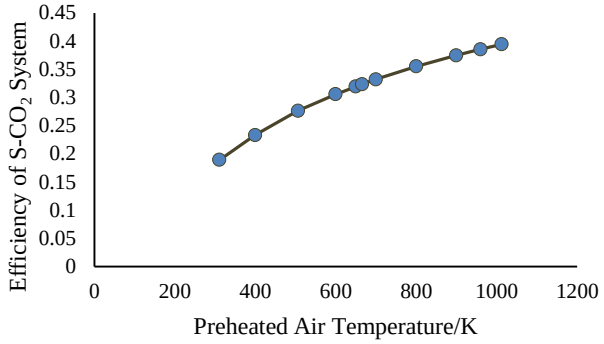

Figure 3. Variation of the cycle efficiency of S-CO_2 system with preheated air temperature.

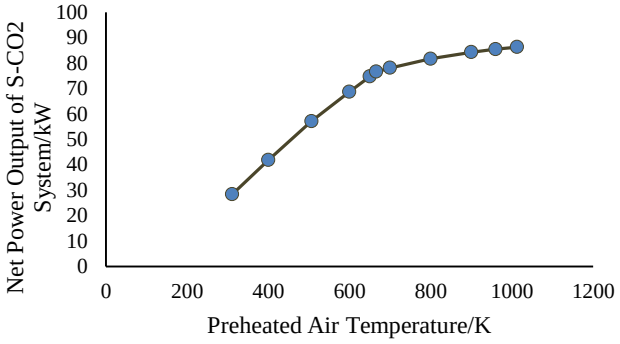

Figure 4. Variation of the net power output of S-CO_2 system with preheated air temperature.

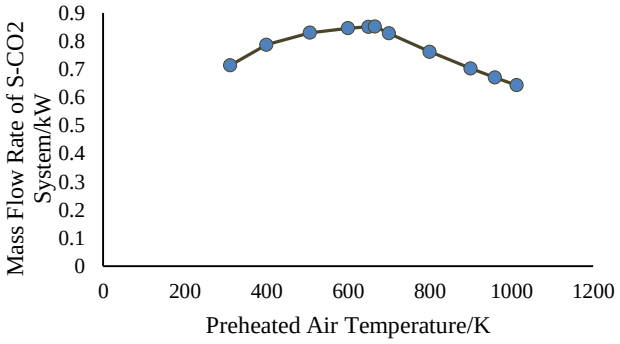

Figure 5. Variation of the working medium mass flow rate of S-CO_2 system with preheated air temperature.

In layout 1, the output power varies with the temperature of the preheated air from HE 1. The variation in the cycle efficiency, the net power output, and the working medium mass flow rate of S-CO_2 system with preheated air temperature are shown in Figure 3, Figure 4, and Figure 5 respectively. With the increment of the preheated air temperature, the heat transfer in HE decreases, resulting in the

increase of the exhaust temperature flowing into the primary HE. As the heat source temperature rises, the cycle efficiency of the S-CO_2 system increases. The net power output of the S-CO_2 system also increases with the increment of preheated air temperature, but the growth slows when the preheated air temperature reaches about 660 K. As the heat source temperature of the S-CO_2 section increases and the mass flow rate remains unchanged, consequently the net power output increases. However, when the preheated air temperature reaches about 660 K, the heat absorption of the S-CO_2 section needs to be cut so that the exhaust from the primary HE can preheat the air and fuel to the required temperature. The efficiency increase of the S-CO_2 system is dominant, therefore the net power output still increases at a lower growth rate. The mass flow rate of the S-CO_2 system first increases and then decreases with the increment of preheated air temperature. With the temperature rise of the heat source, the heat absorption of per unit of working medium increases, while the total heat absorption of the S-CO_2 first increases and then turns down when the preheated air temperature reaches about 660K. Consequently, the mass flow rate of the S-CO_2 system shows a sharp decline with preheated air temperature above 660K.

It's clearly seen that the net power output of the S-CO_2 system reaches the maximum at the preheated air temperature of 1012.75 K. The maximum of the net power output of the S-CO_2 system is 86.36 kW, and the LHV efficiency of the whole system increases by 15.86%.

In layout 2, the power output of the SOFC section remains unchanged, while the power output of the S-CO_2 section increases with the increment of the split ratio. With the split ratio rise, the mass flow rate of the heat source for S-CO_2 section increases. Consequently, the heat absorption and the power output of the S-CO_2 section increase with the increment of the split ratio. However, there is a limit to the split ratio so that the air and fuel can be heated to the required temperature. The net power output of the S-CO_2 system reaches the maximum of 87.86 kW at the highest split ratio of 3.12. The LHV efficiency of the whole system increases by 16.14%.

In layout 3, the exhaust from Ca first flows into the primary HE as the heat source for the S-CO_2 section. In the burner, the exhaust from the primary HE and the An mix in the AB, and extra fuel is added to reach the required temperature. The minimum quantity of the added fuel that meets the specified requirement is 0.00104 kg/s. The net power output of the S-CO_2 system is 96.75 kW, and the LHV efficiency of the whole system increases by 12.14%.

In layout 4, different from layout 1, the S-CO_2 section fully absorbs the heat of the exhaust from the AB. Thus, the exhaust from the primary HE is not able to heat the air and fuel to the required temperature. Extra fuel is added and reacts with the exhaust in an additional burner to raise the temperature. The minimum quantity of the added fuel that meets the specified requirement is 0.00176 kg/s. The net power output of the S-CO_2 system is 116.05 kW, and the LHV efficiency of the whole system increases by 11.84%.

Table 2. The comparison of different hybrid systems.

	Increase of LHV efficiency /%	Number of the HEs	Number of the burners	Increase of power output /kW
SOFC-ORC[11]	6.64	6	1	36.15
Layout 1	15.86	6	1	86.36
Layout 2	16.14	7	1	87.86
Layout 3	12.14	6	1	96.75
Layout 4	11.84	6	2	116.05

The comparison of the proposed four different hybrid systems as well as the SOFC-ORC hybrid system proposed by Ali Volkan Akkaya and Bahri Sahin [11] is shown in Table 2. Compared to the SOFC-ORC hybrid system, all the SOFC-S-CO_2 hybrid systems show significantly better thermal performance. It indicates that the S-CO_2 Brayton cycle can be a promising way for waste-heat recovery of SOFC. Among the four SOFC-S-CO_2 systems, layout 2 shows the highest LHV efficiency. There is an additional HE in layout 2, thus the heat of the exhaust can be more sufficiently utilized. The high efficiency is achieved at the expense of the increase of the system complexity and economic cost. Layout 4 shows the highest power output with an increase of 116.05 kW. The S-CO_2 section in layout 1 and layout 2 just makes partial use of the heat carried by the exhaust from AB. The S-CO_2 section makes full use of the heat carried by the exhaust from Ca in layout 3, while the S-CO_2 section makes full use of the heat carried by the exhaust from AB in layout 4. It is quite clear that both the mass flow rate and the initial temperature of the heat source for S-CO_2 section in layout 4 are higher than that in layout 3. Therefore, the S-CO_2 section of layout 4 shows the highest heat absorption and the highest power output.

To sum up, in layout 1, the exhaust from AB firstly heats the preheated air further, then serves as the heat source for the S-CO_2 section. In layout 2, the exhaust from AB is split in to two parts to serve as the heat source for the S-CO_2 section and heat the air respectively. In layout 3 and layout 4, extra fuel is added to achieve the required temperature. In layout 1, both the efficiency and the power output of the S-CO_2 system increase with the increment of the preheated air temperature. The net power output of the S-CO_2 system reaches the maximum at the preheated air temperature of 1012.75 K. The maximum of the net power output of the S-CO_2 system is 86.36 kW, and the LHV efficiency of the whole system increases by 15.86%. In layout 2, the heat absorption and the power output of the S-CO_2 system increase with the increment of the split ratio. The net power output of the S-CO_2 system reaches the maximum of 87.86 kW at the highest split ratio of 3.1169. The LHV efficiency of the whole system increases by 16.14%. In layout 3, the net power output of the S-CO_2 system is 96.75 kW, and the LHV efficiency of the whole system increases by 12.14%. In layout 4, the net power output of the S-CO_2 system is 116.05 kW, and the LHV efficiency of the whole system increases by 11.84%. It's clearly seen that layout 4 shows the highest output power while layout 2 shows the highest thermal efficiency at the expense of the increase of the system complexity and economic cost.

CONCLUSIONS

In this study, the performance analysis for an indirectly coupled system consisting of an SOFC and a simple recuperated S-CO_2 Brayton cycle is presented. Four system

layouts are selected as candidates. The residual heat carried by the exhaust from the Ca and An of the SOFC are utilized in different ways. The LHV efficiency and the power output of each hybrid system are compared and discussed.

Compared to the SOFC-ORC hybrid system, all the SOFC-S-CO_2 hybrid systems show significantly better thermal performance. It indicates that the S-CO_2 Brayton cycle can be a promising way for waste-heat recovery of SOFC. Among the four SOFC-S-CO_2 systems, layout 2 shows the highest LHV efficiency at the expense of the increase of the system complexity and economic cost. The S-CO_2 section makes full use of the heat carried by the exhaust from AB in layout 4, thus the S-CO_2 section of layout 4 shows the highest heat absorption and the highest power output.

NOMENCLATURE

c_p	Specific heat capacity, kJ/(kg·K)
h	Specific enthalpy, kJ/kg
LHV	Lower hear value, kJ/kg
$\dot{m}$	Mass flow rate, kg/s
P	Pressure, MPa
$\dot{Q}$	Heat transfer rate, kW
T	Temperature, K
Greek symbols	
η	Efficiency
ε	Effectiveness of regenerator
Subscripts	
com	Compressor
HS	Heat source
PHE	Primary heat exchanger
pre-c	Pre-cooler
reg	Regenerator
s	Isentropic
tur	Turbine
Acronyms	
AB	Afterburner
AC	Air compressor
An	Anode
Ca	Cathode
CHP	Combined heat and power
CO	Carbon monoxide
CO_2	Carbon dioxide
FC	Fuel compressor
GT	Gas turbine
H_2	Hydrogen
HE	Heat exchanger
KC	Kalina cycle
M	Mixer
ORC	Organic Rankine cycle
PR	Pre-reformer
S-CO_2	Supercritical carbon dioxide
SOFC	Solid oxide fuel cell

REFERENCES

[1] Stambouli, A. Boudghene, and E. Traversa. "Solid oxide fuel cells (SOFCs): a review of an environmentally clean and efficient source of energy." Renewable and sustainable energy reviews 6.5 (2002): 433-455.

[2] Choudhury, Arnab, H. Chandra, and A. Arora. "Application of solid oxide fuel cell technology for power generation—A review." Renewable and Sustainable Energy Reviews 20 (2013): 430-442.

[3] Ghirardo, Federico, et al. "Heat recovery options for onboard fuel cell systems." International Journal of Hydrogen Energy36.13 (2011): 8134-8142.

[4] Akkaya, Ali Volkan, Bahri Sahin, and Hasan Huseyin Erdem. "An analysis of SOFC/GT CHP system based on exergetic performance criteria." International Journal of Hydrogen Energy 33.10 (2008): 2566-2577.

[5] Winkler, Wolfgang, and Hagen Lorenz. "The design of stationary and mobile SOFC-GT systems." Proceedings 7th UECT (2000).

[6] Winkler, Wolfgang, and Hagen Lorenz. "Design studies of mobile applications with SOFC–heat engine modules." Journal of power sources 106.1-2 (2002): 338-343.

[7] Gholamian, E., and V. Zare. "A comparative thermodynamic investigation with environmental analysis of SOFC waste heat to power conversion employing Kalina and Organic Rankine Cycles." Energy Conversion and Management 117 (2016): 150-161.

[8] Zhang, Shiqi, et al. "An efficient integration strategy for a SOFC-GT-SORC combined system with performance simulation and parametric optimization." Applied Thermal Engineering 121 (2017): 314-324.

[9] Buonomano, Annamaria, et al. "Hybrid solid oxide fuel cells–gas turbine systems for combined heat and power: a review." Applied Energy 156 (2015): 32-85.

[10] Rokni, Masoud. "Thermodynamic analysis of an integrated solid oxide fuel cell cycle with a rankine cycle." Energy conversion and management 51.12 (2010): 2724-2732.

[11] Akkaya, Ali Volkan, and Bahri Sahin. "A study on performance of solid oxide fuel cell‐organic Rankine cycle combined system." International Journal of Energy Research 33.6 (2009): 553-564.

[12] Song, Jian, et al. "Performance improvement of a preheating supercritical CO2 (S-CO2) cycle based system for engine waste heat recovery." Energy Conversion and Management161 (2018): 225-233.

[13] Song, Jian, et al. "Performance analysis and parametric optimization of supercritical carbon dioxide (S-CO2) cycle with bottoming Organic Rankine Cycle (ORC)." Energy 143 (2018): 406-416.

[14] Manjunath, K., et al. "Thermodynamic analysis of a supercritical/transcritical CO2 based waste heat recovery cycle for shipboard power and cooling applications." Energy Conversion and Management 155 (2018): 262-275.

[15] Ahn, Yoonhan, et al. "Review of supercritical CO2 power cycle technology and current status of research and development." Nuclear Engineering and Technology 47.6 (2015): 647-661.

[16] Bae, Seong Jun, et al. "Various supercritical carbon dioxide cycle layouts study for molten carbonate fuel cell

application." Journal of Power Sources 270 (2014): 608-618.
[17] Schöffer, Samuel. "A solid oxide fuel cell-sCO2 Brayton cycle hybrid system: System concepts and analysis." (2017).
[18] Akkaya, Ali Volkan . "Electrochemical model for performance analysis of a tubular SOFC." International Journal of Energy Research 31.1(2007):79-98.
[19] Zhang, Shiqi, et al. "An efficient integration strategy for a SOFC-GT-SORC combined system with performance simulation and parametric optimization." Applied Thermal Engineering 121(2017):314-324.

ACKNOWLEDGMENTS

This study was conducted with the support of National Natural Science Foundation of China (No. 51806118), Foundation of LCP (No. 6142A0501020317).